Available online at www.sciencedirect.com
SCIENCE DIRECT
Polymer 46 (2005) 11288–11293
polymer
www.elsevier.com/locate/polymer

Preparation and characterization of manganese, nickel and cobalt ferrites submicron particles in sulfonated crosslinked networks

L.C. Santa Maria [a,*], M.A.S. Costa [a,*], J.G.M. Soares [a], S.H. Wang [b], M.R. Silva [c]

[a] *Instituto de Química, Universidade do Estado do Rio de Janeiro, Rua São Francisco Xavier, 524, 20550-900 Rio de Janeiro/RJ, Brazil*
[b] *Departamento de Engenharia Metalúrgica e de Materiais, Escola Politécnica, Universidade de São Paulo, Av. Prof. Mello Moraes, 2463, 05508-900 São Paulo/SP, Brazil*
[c] *Instituto de Ciências, Universidade Federal de Itajubá, P.O. Box 50, 37500-000 Itajubá/MG, Brazil*

Received 5 August 2005; received in revised form 2 September 2005; accepted 12 September 2005
Available online 10 October 2005

Abstract

Magnetic submicron particles of $MnFe_2O_4$, $NiFe_2O_4$ or $CoFe_2O_4$ were created in or around the porous sulfonated beads based on poly(styrene-*co*-divinylbenzene) using an in situ inorganic precipitation procedure. The copolymer beads were treated with a mixed iron/cobalt chloride electrolyte and the doped copolymer networks were converted to their oxides by reaction with sodium hydroxide and potassium nitrate in aqueous solution. Energy dispersive X-ray spectroscopy (EDS) coupled to scanning electron microscopy (SEM) allowed the observation of the presence of submicron particles in the 0.1–0.5 μm size range, which chemical microanalysis of emitted X-rays revealed the presence of metal oxide particle, such as nickel, manganese or cobalt iron oxide. The morphological features of the binary material particles have depended on the ferrite type. All beads have presented dispersed and agglomerated submicron particles of ferrite located on their surface and inner part as well. Magnetization data of the microbeads showed good ferromagnetic behavior.

Keywords: Polymer; Magnetic properties; Ferrite

1. Introduction

Magnetic separation has been widely applied to various aspects in biotechnology and biomedical engineering, such as cell separation [1], pollutant removal [2], water treatment [3], cell labeling [4], enzyme immunoassaying [5], drug targeting [6], enhancement of magnetic resonance imaging [7], etc. Actually, magnetic separation is relatively rapid and easy, cost helpful and highly efficient. To make full use of the magnetic separation technology, magnetic carriers with good properties are indispensable. Many different techniques have been developed for magnetic particle preparations [8]. The porous copolymer networks based on poly(styrene-*co*-divinylbenzene) can be rendered polar by sulfonation reactions that do not affect the beads mechanical properties. In addition, by using sol–gel reactions of metal alkoxides it is possible that sulfonated copolymers could perform as reaction patterns in the formation of organic–inorganic submicron structured hybrid materials domain-targeted in situ within themselves [9].

The submicron particles of metal oxides such as soft ferrites are particularly important since they are relatively inert and their properties can be tailored by chemical manipulations [10]. The magnetic characteristics of ferrites are strongly affected when the particle size approaches the critical diameter, below which each particle is a single magnetic domain. Nevertheless, the tendency of isolated nanostructures to turn into bigger clusters during the synthesis had denoted a significant difficulty for size control. Alternatively, mesoporous-based polymer templates have been efficiently employed to host chemical reactions, not only avoiding nanoparticle clustering but also providing stable frameworks against chemical degradation [10,11].

In this paper, we describe the synthesis and characterization of magnetic beads that were created by the precipitation of $MnFe_2O_4$, $NiFe_2O_4$ or $CoFe_2O_4$ submicron particles hosted in sulfonated poly(styrene-*co*-divinylbenzene) microspheres with different porosities aiming to achieve materials with good magnetic properties.

* Corresponding authors. Fax: +55 21 2587 7227.
E-mail addresses: lcsm@uerj.br (L.C. Santa Maria), masc@uerj.br (M.A.S. Costa).

0032-3861/$ - see front matter © 2005 Elsevier Ltd. All rights reserved.
doi:10.1016/j.polymer.2005.09.055

2. Experimental part

2.1. Materials

Styrene (STY) and divinylbenzene (DVB, grade of 45% of DVB isomers, containing a mixture of DVB and ethylvinylbenzene) were kindly donated by Petroflex and Niriflex, respectively and used as received. α,α′-Azo-bis-isobutyronitrile (AIBN, donated by Metacril, Brazilian Co.) was purified by recrystallization from methanol. 2-Hydroxyethyl-celullose (HEC, Cellosize QP-100MH) was donated by Union Carbide and used as received. The commercial resins were kindly supplied by Rohm and Haas Co., namely Amberlite IR120H (sulfonic gel type resin, exchange capacity = 1.8 mmol/g of resin, data informed by supplier) and Amberlyst 15WET (mesoporous sulfonic resin, exchange capacity = 1.7 mmol/g of resin, $S_a = 53\ m^2/g$, $D_p = 300$ Å, $V_p = 0.4$ ml/g, data informed by supplier). The other reagents were commercially purchased, gelatin, sodium chloride, propanone, nickel chloride, cobalt chloride, manganese chloride, ferrous sulphate, potassium nitrate, sodium hydroxide, 1,2-dichloroethane, acetic anhydride, methanol, isopropanol, toluene, concentrated sulfuric acid and glacial acetic acid all P.A. degree, and spectroscopic potassium bromide (Vetec Química Fina Ltda, Brazil) were used as received. Aqueous solutions were prepared using distilled deionized water.

2.2. Copolymer synthesis

The aqueous suspension copolymerization of STY/DVB was carried out in a 1L, three-necked, round-bottomed flask glass reactor fitted with mechanical stirrer, reflux condenser with a silicon oil seal at its top. Aqueous phase (AP) was composed by gelatin (0.1 wt% of AP) and 2-hydroxyethyl-celullose (0.1 wt% of AP) and NaCl (2.0 wt% of AP). The organic phase (OP) was composed by STY 3 (11 ml), DVB (57 ml), toluene (20 ml) and *n*-heptane (80 ml) employed as diluents and AIBN used as initiator (1.0 mol% of monomers). OP was added slowly to AP previously prepared under stirring at room temperature, employing AP/OP ratio = 4/1. These two phases were maintained under stirring (300 rpm) at room temperature during 10 min. Hence the suspension copolymerization system was kept under stirring at 65 °C during 24 h. The resin beads was thoroughly washed with warm water (eight portions of 500 ml) and with propanone (three portions of 500 ml) and dried at 60 °C.

2.3. Copolymer beads sulfonation

The copolymer beads (5 g) were previously swollen with 1,2-dichloroethane (120 ml) during 24 h in a three-necked, round-bottomed flask glass reactor. The concentrated sulfuric acid (7 ml) was added slowly, under mechanical stirring, at room temperature. The system was warmed slowly until 90 °C and kept under stirring during 2 h. The sulfonated beads were filtered off, washed with warm water, then extracted with methanol in a Soxhlet (around 30 cycles) and finally dried at 60 °C.

2.4. Ion exchange and metal oxide reaction precipitation

The ion exchange was carried out by using 3 g of resin beads (namely synthesized resin—SR, Amberlyst 15WET or Amberlite IR120H) immersed in an aqueous solution containing Fe^{2+} (50 ml at 0.25 M) and Mn^{2+} or Ni^{2+} or Co^{2+} ions (100 ml at 0.25 M). Two drops of concentrated sulfuric acid was added to reduce the pH. The resin was kept in contact during 2 h. Then the beads were filtered off, washed thoroughly with distilled deionized water. The resin containing Fe^{2+} and Mn^{2+} (Ni^{2+} or Co^{2+}) ions was treated with 100 ml of an aqueous solution of KOH and KNO_3, previously warmed to 90 °C. This mixture was kept under stirring during 5 min. Finally the beads were thoroughly washed with distilled deionized water and propanone and dried at 60 °C. The iron content was determined by colorimetric method.

2.5. Magnetic, morphological and area surface characteristics

Magnetization curves were carried out in an AGGPAR 4500 ibrating sample magnetometer (VSM), calibrated against a cylindrical nickel standard at room temperature (cycle time = 1 s and hystereses cycle time = 10 min). Philips XL-30 scanning electron microscope was used for textural analysis of microbead surfaces and inner microstructures. The presence of metal particles was confirmed by energy dispersive X-ray spectrometry using an EDAX microprobe. Preparation of the samples for imaging and analysis by SEM was straightforward. The samples were dispersed on a conductive tape and submitted to gold sputtering to make them conductive prior to the analyses. The specific surface area (in m^2/g), average pore diameter (Å) and pore volume in the dry state (ml/g) were determined by the BET and BJH methods respectively from low-temperature nitrogen adsorption isotherms (ASAP Micromeritics 2000) at 77 K using a high-vacuum volumetric apparatus. The samples were degassed at 100 °C/1 mPa for 3 h.

3. Results and discussion

In order to prepare a STY/DVB resin with porous structures, suspension copolymerization was carried out in the presence a mixture of solvents as porogenic agent. It was observed that 76% of this material had particle sizes between 300–1180 μm. The copolymer beads have presented bulk density of 0.3 g/cm^3. Moreover, the swelling degree in water, toluene and 1,2-dichloroethane were 0, 10 and 20%, respectively. These low values of bulk density and swelling degree indicate that copolymer beads are porous. Fig. 1 shows a SEM micrograph of synthesized resin (SR). As it can be confirmed, the copolymer beads present porous structure.

After sulfonation, the beads became dark brown and swelled better in polar solvents (30% swelling in water) compared to the unmodified resin, indicating the presence of hydrophilic groups ($-SO_3H$). The attached sulfonyl groups of

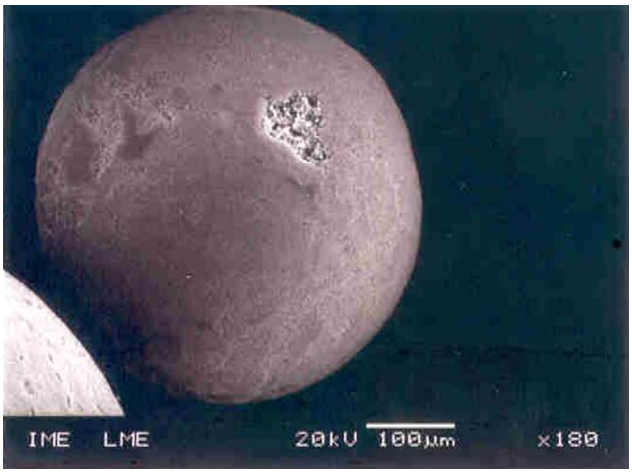

Fig. 1. SEM Micrograph of the synthesized resin (SR) based on styrene and divinylbenzene.

the synthesized resin based on styrene–divinylbenzene were identified with strong stretching band of S=O in the range 1300–1000 cm^{-1}, whereas the broad stretching band near 3500–3300 cm^{-1} resulted from the hydroxyl groups of $–SO_3H$ and absorbed water into the resin [12,13]. The microscopic analysis has shown that the sulfonation process did not modify the morphological characteristics of resin beads.

The ferrites synthesis was evaluate on three copolymer networks with different porous structure, namely Amberlite IR120H (sulfonic gel-type resin—mostly without pores), which produced 1IR, 2IR and 3IR resins containing Mn, Ni and Co ferrites, respectively; Amberlyst 15WET (mesoporous sulfonic resin, $S_a=53$ m^2/g, $D_p=300$ Å, $V_p=0.4$ ml/g), which produced 1WET, 2WET and 3WET resins containing Mn, Ni and Co ferrites, respectively; and sulfonic highly crosslinked resin based on styrene with divinylbenzene synthesized by ourselves (mesoporous resin, $S_a=92$ m^2/g, $D_p=210$ Å, $V_p=0.3$ ml/g), which produced 1SR, 2SR and 3SR resins containing Mn, Ni and Co ferrites, respectively. The process for obtaining ferrites micro sized particles ($MnFe_2O_4$, $CoFe_2O_4$ or $NiFe_2O_4$) preparation follows the reactions given below and it was carried out in an aqueous medium.

$$Mn^{2+} + 2Fe^{2+} + 8OH^- \xrightarrow{NO_3^-/\Delta} MnFe_2O_4 + 4H_2O$$

$$Co^{2+} + 2Fe^{2+} + 8OH^- \xrightarrow{NO_3^-/\Delta} CoFe_2O_4 + 4H_2O$$

$$Ni^{2+} + 2Fe^{2+} + 8OH^- \xrightarrow{NO_3^-/\Delta} NiFe_2O_4 + 4H_2O$$

The literature has pointed out that the size of ferrite nanoparticles is restricted to a maximum of about 90 Å [14]. This particle size is smaller than diameter size of the bead pores. Following the model (Fig. 2) considered by Ziolo [15], the ferrite particles should be formed through ions fixation and particle precipitation around and/or within the beads macrostructure, as depicted in Fig. 2.

A general view of the synthesized spherical beads scattered on the sample holder shows small $CoFe_2O_4$ particles on their surfaces, as can be seen in Fig. 3. The ferrite and polymer regions were analyzed by backscattered electrons detector. Since the contrast in this kind of image formation is obtained by differences in the atomic number of the elements in the sample, it was possible to distinguish the ferrite distribution on the microspheres. Then, EDS microanalysis was employed to determine the constitution of the ferrite dispersed in the polymeric matrix. In addition, all kind of ferrites particles could be detected on the surface as well as inside fissures of the beads. The quantitative analyses of the EDS spectra, taken from some samples in high-resolution SEM, yielded stoichiometric composition of nickel ferrite thus in situ formed was in chemical equilibrium, allowing achievement of nearby stoichiometric composition [11].

Fig. 4 shows that the beads surface presents two different features. It is possible to see small particles of ferrite randomly dispersed on the bead surface (Fig. 4(a)) and inner part (Fig. 4(d)), while the same characteristic could not be observed on the bead surface of 2WET (containing $NiFe_2O_4$, Fig. 4(b)). Actually, some beads present few clusters of nickel ferrite particles on preferential regions of their surfaces (internal and external). Based on these initial experiments we propose that it could be due to the difference in $–SO_3H$ group concentration, which could influence the ferrite formation process. As it is shown in Fig. 4(d), the $CoFe_2O_4$ particles were characterized by flake about 1 µm in size located in the internal fissure present in the original commercial resin (15WET).

Fig. 5 shows the magnetic hysteresis loops for the prepared resins. The hysteresis loops were measured to determine

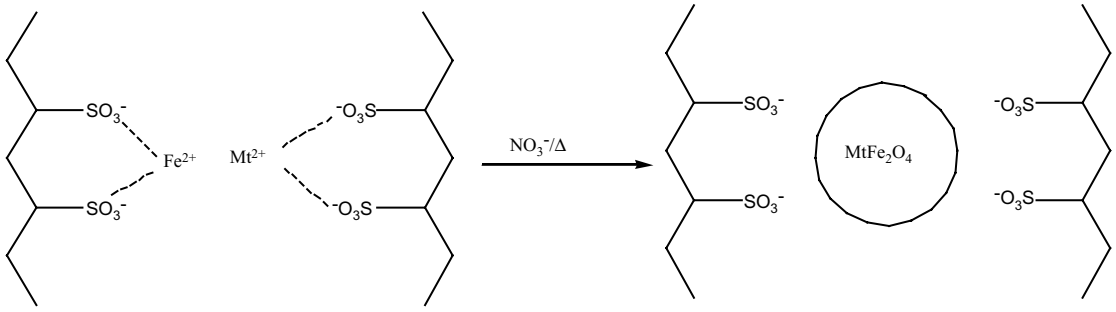

ions fixed on the resin macrostructure

ferrite particle formed in the resin macrostructure

Fig. 2. Model for the ferrite particles formation around and/or within the beads macrostructure (Mt=Mn, Ni or Co).

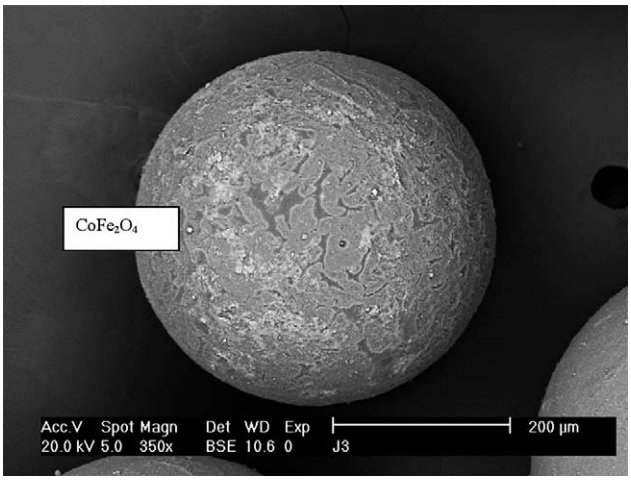

Fig. 3. Scanning electron micrograph of 3SR (sulfonic synthesized resin) bead containing $CoFe_2O_4$.

parameters such as the saturation magnetization (M_S), remanent saturation (M_R) and coercivity (H_C) for all binary materials, which are summarized on Table 1. The coercivity (H_C) is the reverse field required to reduce the magnetization to zero from saturation. The magnitude of H_C is affected by the particle size and homogeneity of each material [8]. The coercivities of the synthesized binary materials are between 22.580 and 36.739 kA m^{-1}. Generally all materials have a strong attraction to a magnetic bar, especially the 1SR, 2SR, 3SR and 1WET, 2WET, 3WET resin sets. The IR set resins had presented a weak attraction to a magnet. Comparing the hysteresis loops of the resin sets (IR, WET and SR), it is possible to note that the resins containing $MnFe_2O_4$ (1IR, 1WET and 1SR) were magnetically softer materials than the others. The $MnFe_2O_4$-based resin has presented the highest values of M_R and M_S (Table 1).

The magnetization hysteresis loops of all the resins (Fig. 5) are typical for ferromagnetic materials [16]. In this work, the magnetic materials present submicron particles of ferrites, which are strongly magnetized phase anchored homogenously on the beads surface (non-ferromagnetic phase based on sulfonated styrene–divinylbenzene copolymers). Table 1 shows that the values of iron content are almost same therefore, the formed ferrite amount was independent on the copolymers beads porosity.

As can been noted in Fig. 5(a), all the magnetic materials based on Amberlite IR120H resin have presented lower magnetization than those prepared with Amberlyst 15WET and sulfonated SR resins. The magnetization behavior of the resins as a function of field strength clearly shows the influence of the distribution of ferrite particles on the magnetic properties (Fig. 4). The difference of M_S measurements (lower M_S values for IR resins set) may be explained by the agglomeration of their particles on the beads surface. This result could be explained by the higher population of $–SO_3H$ groups on the external surface of the IR resin (gel-like resin) compared to the others (WET and sulfonated SR), which are porous materials.

An interesting feature of M_R/M_S ratio was also noted (Table 1). The IR samples' set has presented lower values of M_R/M_S ratio (range 0.14–0.20) compared to those observed for WET and SR resin sets (0.40–0.61 range). These lower M_R/M_S ratio values in IR resin samples indicate an appreciable fraction of superparamagnetic particles at this temperature (300 K).

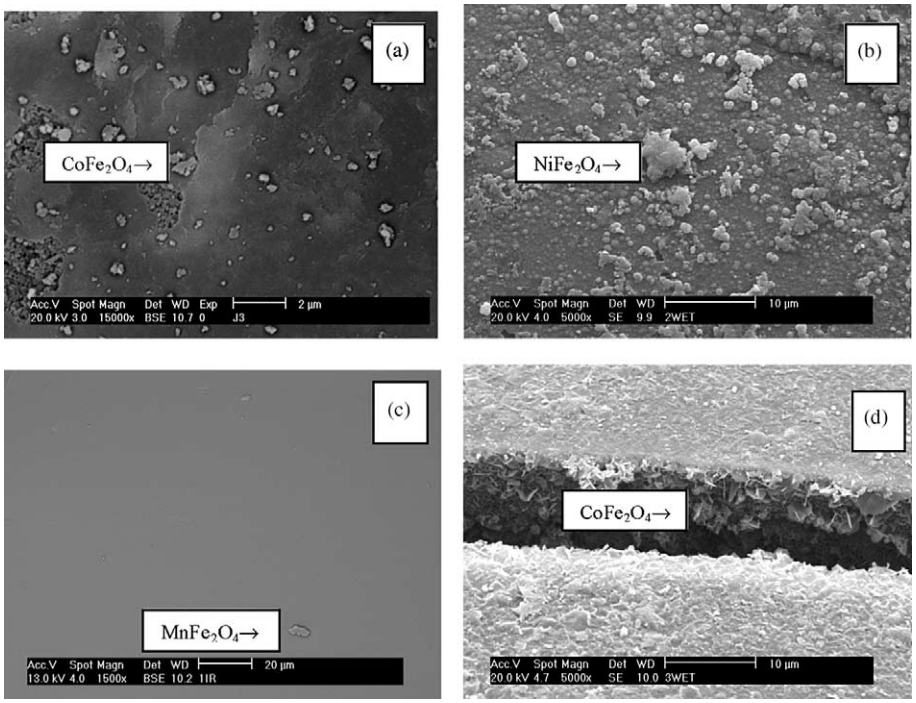

Fig. 4. SEM micrographs of resins based on ferrites prepared on copolymers beads (external part) (a) 3SR resin (containing $CoFe_2O_4$); (b) 2WET resin (containing $NiFe_2O_4$); (c) 1IR resin (containing $MnFe_2O_4$) and (d) 3WET (external part and a fissure on the surface bead containing $CoFe_2O_4$).

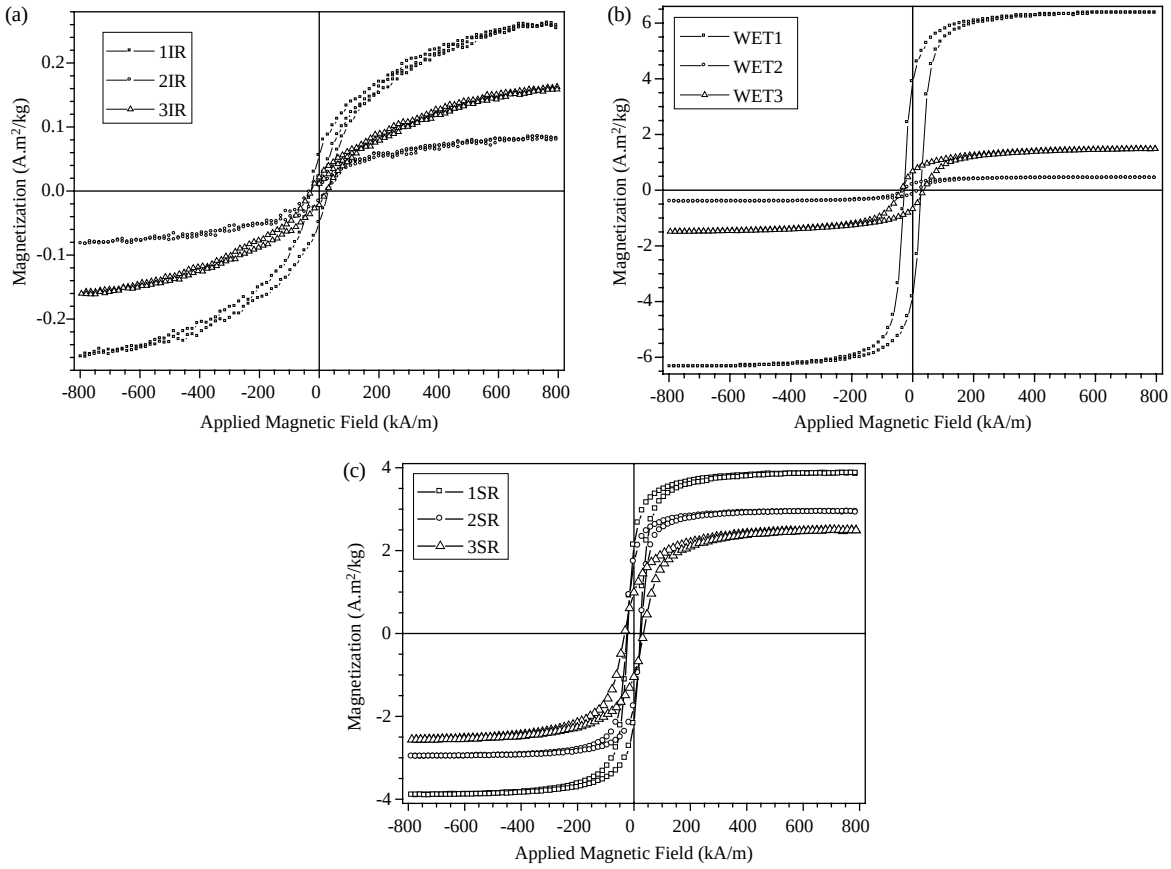

Fig. 5. Variation of magnetization with the applied field at 300 K (hysteresis loops) (a) ferrites on Amberlite IR120H resin (1IR, $MnFe_2O_4$; 2IR, $NiFe_2O_4$; 3IR, $CoFe_2O_4$); (b) ferrites on Amberlyst 15WET resin (1WET, $MnFe_2O_4$; 2WET, $NiFe_2O_4$; 3WET, $CoFe_2O_4$); (c) ferrites on synthesized resin (1SR, $MnFe_2O_4$; 2SR, $NiFe_2O_4$; 3SR, $CoFe_2O_4$).

Table 1
Iron content, magnetization values (M_S and M_R), coercive forces (H_C) and ratio of remanent induction to saturation magnetization (M_R/M_S) at 300 K for the synthesized resins

Resins	Fe content[a] (%wt/wt)	H_C (kA/m)	M_S (A m^2/kg)	M_R (A m^2/kg)	M_R/M_S
1IR	7.9	28.388	0.25895	0.05260	0.20
2IR	7.5	28.905	0.082096	0.01919	0.23
3IR	7.7	26.411	0.16051	0.02168	0.14
1WET	8.4	27.533	6.3507	3.8656	0.61
2WET	6.4	24.011	0.42882	0.18045	0.42
3WET	6.0	36.739	1.4763	0.67716	0.46
1SR	nd	22.580	3.8829	2.1522	0.55
2SR	8.3	25.555	2.9516	1.7458	0.59
3SR	8.6	34.026	2.5300	1.0199	0.40

nd, not determined; H_C, coercivity; M_S, saturation magnetization; M_R, remanent magnetization; 1IR, 2IR, 3IR—resins containing $MnFe_2O_4$, $NiFe_2O_4$ or $CoFe_2O_4$ anchored on Amberlite IR120H, respectively; 1WET, 2WET, 3WET—resins containing $MnFe_2O_4$, $NiFe_2O_4$ or $CoFe_2O_4$ anchored on Amberlyst 15WET, respectively; 1SR, 2SR, 3SR—resins containing $MnFe_2O_4$, $NiFe_2O_4$ or $CoFe_2O_4$ anchored on synthesized sulfonic resin, respectively.

[a] Determined by colorimetric method.

Although the hysteresis loop widths of these resins are broad (high H_C values range 26.411–28.905 kA m^{-1}), the M_R/M_S ratios are comparable with superparamagnetic materials. These values meet the requirements for coil core materials, assuring high magnetic permeability and minimal energy losses [17]. This result could be explained by the ferrite particles portion of smaller size hosted on this copolymer (Amberlite IR120H) compared to the resins obtained from others resins (Amberlyst 15WET and synthesized sulfonic copolymer).

4. Conclusions

We have investigated the anchorage of Mn, Ni and Co ferrites on the network structure of polymer particles. The studies suggest an influence of sulfonic copolymer networks porosity on ferrite particles' setting. The ferrite content was independent on the copolymers beads porosity. These binary materials based on polymeric matrix containing submicron sized particles of Mn, Ni or Co ferrites have presented good

ferromagnetic properties, which are dependent on the ferrite particles size, distribution and agglomeration of anchored ferrite particles on the copolymer pearls surface.

Acknowledgements

We thank to CNPq, FAPERJ and CETREINA/UERJ for financial support. We also wish to express their thanks to Instituto Militar de Engenharia for SEM characterization, to Petroflex, Nitriflex and Metracril do Brasil for monomers and initiator donations, to Instituto de Física/UFRJ for magnetic measurements.

References

[1] Porter J, Pickup RW. J Microbiol Methods 1998;33(3):221–6.
[2] Imai A, Fukushima T, Matsushige K, Kim YH, Choi K. Water Res 2002; 36(4):859–70.
[3] Johnson CJ, Singe PC. Water Res 2004;38(17):3738–50.
[4] Xie X, Zhang X, Zhang H, Chen D, Fei W. J Magn Magn Mater 2004; 277(1–2):16–23.
[5] Koneracká M, Kopcansky P, Timko M, Ramchand CN. J Magn Magn Mater 2002;252(1–3):409–11.
[6] Gupta PA, Hung CT. Life Sci 1989;44(3):175–86.
[7] Parkin SSP, More N, Roche KP. Phys Rev Lett 1990;64(19):2304–7.
[8] Santa Maria LC, Leite MCAM, Costa MAS, Ribeiro JMS, Senna LF, Silva MR. Mater Lett 2004;58:3001–6.
[9] Rajan GS, Stromeyer SL, Mauritz KA, Miao G, Mani P, Shamsuzzoha M, et al. J Magn Magn Mater; in press.
[10] Morais PC, Azevedo RB, Rabelo D, Lima ECD. Chem Mater 2003; 15(13):2485–7.
[11] Kale A, Gubbala S, Misra RDK. J Magn Magn Mater 2004;277:350–8.
[12] Oliveira AJB, Aguiar AP, Aguiar MRMP, Santa Maria LC. Mater Lett 2005;59:1089–94.
[13] Lambert JB, Shurvell HF, Lightner D, Cooks RG. Introduction to organic spectroscopy. New York: Macmillan Publishing Co.; 1987.
[14] Felinto MCFC, Parra DF, Lugão AB, Batista MP, Higa OZ, Yamaura M, et al. Nucl Instrum Methods Phys Res B 2005;236(1–4):495–500.
[15] Ziolo RF, Giannelis EP, Weinstein BA, O'horo MP, Ganguly BN, Mehrotra V, et al. Science 1992;257(5067):219–23.
[16] Chen L, Yang WJ, Yang CZ. J Mater Sci 1997;32:3571–5.
[17] Skolyszewska B, Tokars W, Przybylski K, Kakol Z. Physica C 2003;387: 290–4.